Nanopatterning

DOI: 10.1002/ange.201006544

Self-Assembled Arrays of Dendrimer–Gold-Nanoparticle Hybrids for Functional Cell Studies**

Anders Lundgren, Yvonne Hed, Kim Öberg, Anders Sellborn, Helen Fink, Peter Löwenhielm, Jonathan Kelly, Michael Malkoch, and Mattias Berglin**

Engineered surfaces with nanoscale features of gold on silicon or glass have recently been used to improve the understanding of adhesion-mediated environmental sensing of cells. Often such surfaces present a cell-binding ligand, such as arginine–glycine–aspartic acid (RGD) peptide motifs, at controlled intramolecular distances on an inert background surface such as polyethylene glycol (PEG).[1] The adhesion mechanism of macromolecular ligands in which direct interaction with cells is nonspecific is not known and the cell response is dictated by the type and the concentration of proteins adsorbed from solution.[2] Dendrimers may increase the availability and multivalency of cell-interacting ligands as a consequence of their branched shape and inherently high concentration of end groups.[3] It is therefore interesting to examine the eventual effect of the macromolecular architecture on the cell viability by the controlled reduction of ligands on a surface. Herein, we demonstrate the fabrication of self-assembled macromolecular hybrid arrays in which the relative position of two anionic macromolecules of different architectures—a carboxy-functionalized dendrimer and a linear polymer—is straightforwardly controlled on a PEG surface. We also show how the interaction of primary human endothelial cells with these surfaces is modulated by the molecular spacing and how protein binding to the macromolecular arrays can be evaluated by using a standard surface plasmon resonance (SPR) technique.

Self-assembled, short-range-ordered Au nanoparticle (NP) arrays were used as a versatile template to arrange polymeric entities at the nanometer scale (Figure 1 a). This

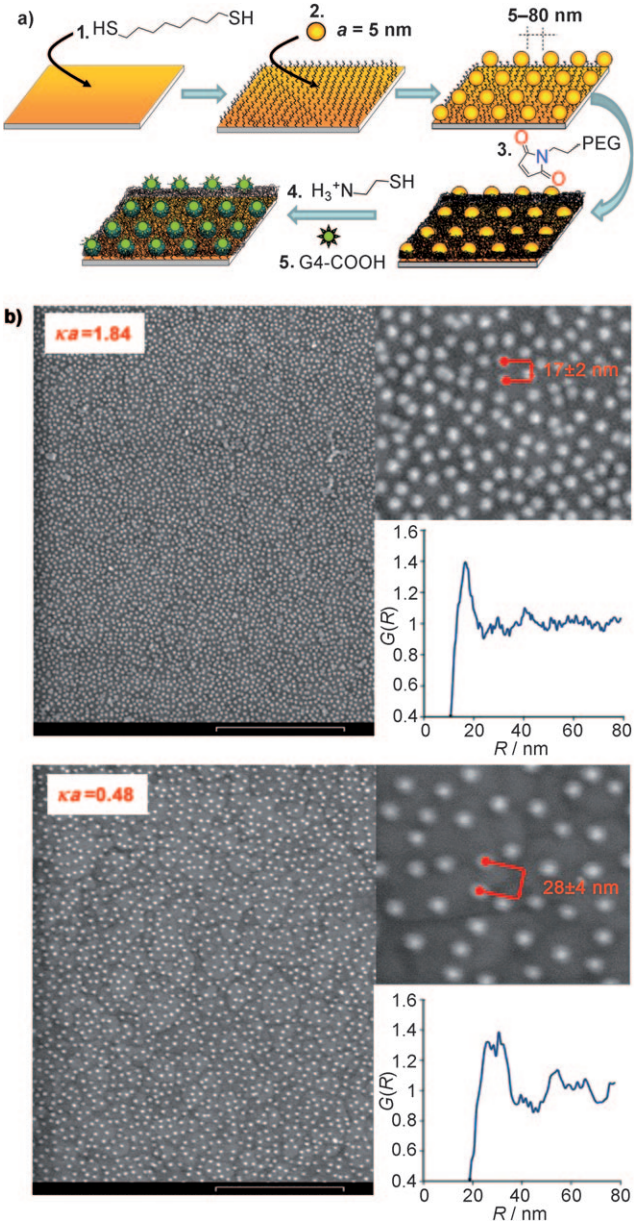

Figure 1. a) The self-assembly protocol in which formation of the octanedithiol (**1**) monolayer is followed by immobilization of NPs **2** of $a = 5$ nm radius and reaction with malemide-functionalized PEG **3**. The fabrication of the polymer hybrid array ends with modification of the NP template with cysteamine (**4**) and immobilization of the synthesized G4-COOH dendrimer **5**. b) The interparticle distance as determined by SEM under two deposition conditions, $\kappa a = 1.84$ and $\kappa a = 0.48$, together with the radial distributions (scale bars = 500 nm).

[*] A. Lundgren, Dr. M. Berglin
Cell and Molecular Biology, Interface Biophysics
Göteborg University (Sweden)
E-mail: mattias.berglin@cmb.gu.se
Y. Hed, K. Öberg, Dr. M. Malkoch
Royal Institute of Technology, School of Chemistry
and Chemical Science, Coating Technology (Sweden)
E-mail: malkoch@kth.se
Dr. P. Löwenhielm, Dr. J. Kelly
Mölnlycke Health Care AB
Box 130 80, 40252 Göteborg (Sweden)
Dr. A. Sellborn, Dr. H. Fink
Department of Surgery, Sahlgrenska University Hospital
Göteborg University (Sweden)

[**] We thank the Swedish Research Council (VR) Grants 2006-3617 (M.M.) and VR 2009-5398 (M.B.), the Willhelm Beckers Jubileumsfond (Y.H.), and the VINNOVA SAMBIO. Prof. Hans Elwing is acknowledged for helpful discussions.

Supporting information for this article is available on the WWW under http://dx.doi.org/10.1002/anie.201006544.

experimentally simple approach, based on sequential steps of chemical self-assembly, offers a straightforward, nonlithographic method to modify large flat or curved substrates and it may, therefore, be used for the realization of functional nanopatterned devices.

Charge-stabilized gold nanoparticles [radius $a = (5 \pm 0.5)$ nm] were synthesized by reduction of a gold salt[4] with citrate and tannic acid and subsequent adsorption under electrostatic control to gold substrates premodified with a self-assembled monolayer of octanedithiol (**1**) as described earlier.[5] By keeping a constant NP concentration of 5×10^{-8} M, but altering the ionic strength of the gold sol, NPs will bind on the surface at a distance corresponding to approximately two times the double layer thickness κ^{-1} from each other. In our experience, this strategy can be used to position particles with a 5 nm radius at distances ranging from 5 to 80 nm. For the fabrication of polymer arrays, NPs were adsorbed under two different conditions, 10 mM and 0.625 mM citric buffer at a pH 4, which correspond to $\kappa a = 1.84$ and $\kappa a = 0.48$, respectively. The mean center-to-center interparticle distances were determined by scanning electron microscopy (SEM) to be 17 and 28 nm, respectively, by calculation of radial distributions $g(R)$, where R is the distance between two particle centers (Figure 1b). These values correspond to a nanoparticle coverage θ of approximately 30 and 10%, respectively.

The thiolated area between the NPs was pegylated with malemide-functionalized polyethylene glycol (M-PEG, average molecular mass 5000 g mol^{-1}) **3** to generate protein and cell-repellent properties. The double bond of the malemide group undergoes an alkylation reaction with the free sulfhydryl group to yield a stable thioether bond. The chemical reaction was verified with a quartz crystal microbalance with dissipation (QCM-D; see the Supporting Information) and tapping mode (TM) AFM (Figure 2). The NPs were made positively charged by using cysteamine (**4**) prior to immobilization of two carboxy-functionalized macromolecules with similar charge but with distinctly different architectures. Polyacrylic acid (PA-COOH) with an average molecular weight of 5100 g mol^{-1} and 54 carboxy groups was chosen as a linear polymer with a random coil conformation. In contrast, the nontoxic, water-soluble, and commercially available fourth generation bis(methylol)propionic acid (bis-MPA) dendrimer (PFD-TMP-G4-OH, Figure 3)[6] was identified as a second polymer scaffold.[7] This dendrimer is highly branched, globular at higher generations, and exposes 48 peripherial hydroxy end groups. The development of a facile and robust synthetic route that results in complete carboxylation of all 48 OH groups was required to introduce the negative charge. While a simple ring-opening reaction of succinic anhydride was utilized in earlier reports to obtain carboxylated polymers,[8] the monodisperse structure of the dendrimers requires unprecedented control over the reaction conditions. The synthesis of the anhydride-activated 4-(benzyloxy)-4-oxobutanoic acid **8** was therefore targeted since the benzyloxy-protected carboxylic group can efficiently react with the dendritic moiety through typical anhydride reactions (Scheme 1).[9] The anhydride was produced on a 200 g scale,

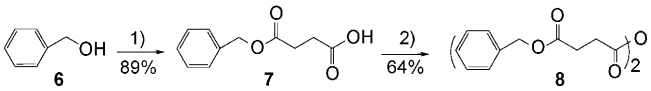

Scheme 1. Synthesis of 4-(benzyloxy)-4-oxobutanoic acid **8**. 1) Succinic anhydride and 4-dimethylaminopyridine (DMAP) in dichloromethane. 2) Dicyclohexylcarbodiimide (DCC) in CH_2Cl_2 at 0 °C.

and successfully reacted with PFD-TMP-G4-OH. The isolated benzyloxy-protected dendrimer intermediate was further deprotected using a Pd/C-catalyzed hydrogenolysis reaction. The progress of the reaction was monitored continually by NMR spectroscopy and MALDI-TOF analysis, and the final carboxylated product—the fourth generation bis-MPA dendrimer PFD-TMP-G4-COOH$_{48}$ **5** ($M = 10\,163$ g mol^{-1}, also denoted G4-COOH)—was isolated in a high total yield of 93% (Figure 3a).

The electrostatic immobilization of the dendrimer as a function of NP coverage was monitored using QCM-D (Figure 3b). The adsorbed mass, around 60 ng cm^{-2} for 30% NP coverage, corresponds adequately to a 1:1 stoichiometric ratio between the NPs and immobilized dendrimer. No adsorption of the dendrimer could be observed on the negative control surface (M-PEG) or on NPs not treated with cysteamine **4**. The presence of the dendrimer was further verified by monitoring the concentration of a molecular mass fragment at $m/z = 117$—which could be assumed to be rather specific because of the molecular structure of the dendrimer (Figure 3c)—by chemical mapping using time-of-flight secondary ion mass spectrometry (TOF-SIMS).

Primary human saphenous vascular endothelial cells (PHSVEC) were employed to evaluate the effect of anionic nanodomains expressed by two inherently different polymer architectures. This cell type lines the inside of blood vessels and when viable expands laterally, thereby acquiring a cobblestone-like appearance. After 24 h of incubation, the cells were fixed with formaldehyde and stained with 4′,6-diamidino-2-phenylindole (DAPI), Vinculin, and Alexa 488 conjugated phalloidin. Representative fields of view as observed by confocal laser scanning microscopy (CLSM) are shown in Figure 4a–f. A trend of decreasing numbers of cells and decreasing size of cells with larger interparticle separation was observed (Figure 4g,h). Similar trends have been observed with RGD-presenting arrays, but morpholog-

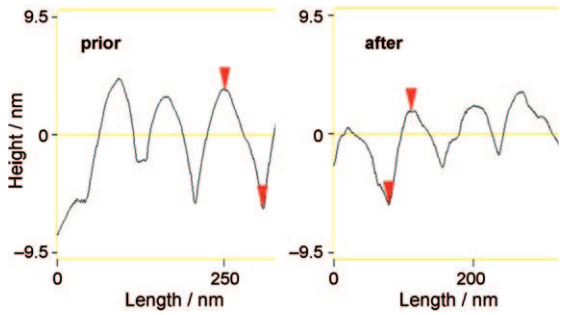

Figure 2. TM-AFM height image prior to and after reaction with M-PEG.

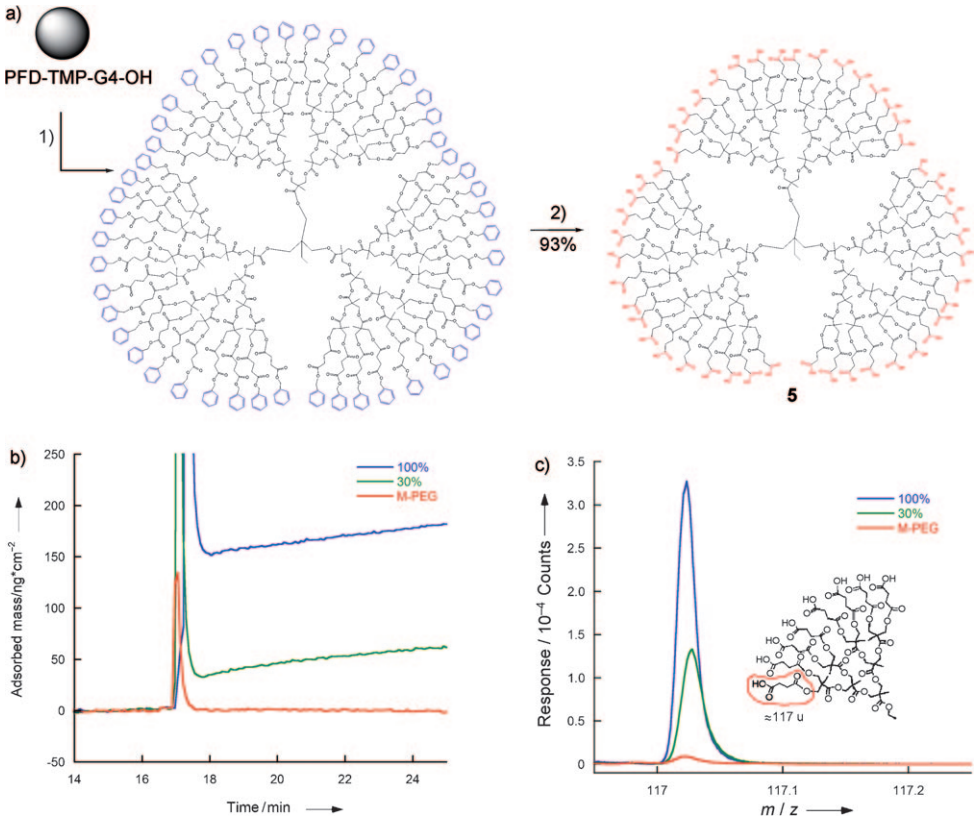

Figure 3. a) Synthesis of the carboxy-terminated G4-dendrimer **5**. 1) **8**, DMAP, and pyridine in CH_2Cl_2. 2) Deprotection using Pd/C-catalyzed hydrogenolysis in EtOAc/MeOH. b) The immobilization of the dendrimer, which starts at $t = 17$ min, adequately corresponds to the nanoparticle coverage determined by QCM-D. c) The presence of the dendrimer was verified by chemical mapping using TOF-SIMS.

ical changes then occurred at larger ligand separations.[1e–g] Interestingly, a distinct difference between the dendrimer and the linear counterpart was displayed at 30% surface coverage. The dendrimer attracted 100% more cells which were twice as large as cells on PA-COOH. These results suggest that the dendrimer-functionalized surface adsorbs and makes bioavailable a larger number of cell-interacting ligands than the linear counterpart when applied at similar surface coverage ratios. This subtle difference in the cell response would be unnoticed without the use of a macromolecular array that gives precise control over the ligand concentration. Very few cells (< 5 per mm^2) were found on the fully pegylated (negative control) surface.

Since little direct interaction between the negatively charged polymers and the negatively charged cells is anticipated, interactions will be mediated by proteins in the

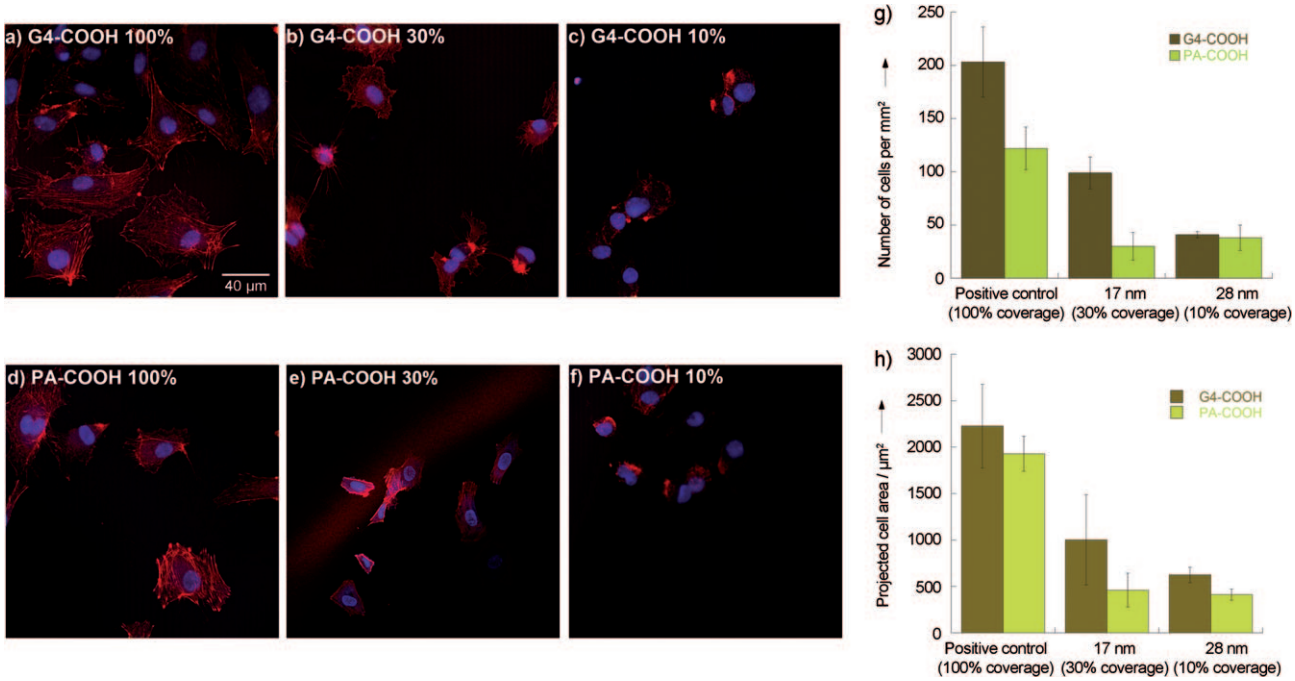

Figure 4. Representative confocal laser scanning microscopy (CLSM) images of cells attached to G4-COOH (a–c) and PA-COOH (d–f) functionalized surfaces. The number of cells and the average projected area are shown in (g) and (h), respectively.

cell media which bind to the surface-immobilized macromolecules. As an example of such proteins we chose to characterize the binding of endothelial cell growth factor (ECGF, also referred to as aFGF or FGF-1) and albumin directly on macromolecular arrays prepared on commercial gold substrates for SPR analysis. In this way, protein binding can be directly related to the number of macromolecules on the surface.

Recombinant human ECGF (MW 17 kDa) was injected at concentrations ranging from 5 to 200 nM onto the array surfaces by using a Biacore system. The injection of 200 nM (3.4 $\mu g\,mL^{-1}$) ECGF gave rise to large binding both on the dendrimer- and the PA-COOH-modified arrays, but no proteins bound to the control surface (M-PEG; Figure 5). It

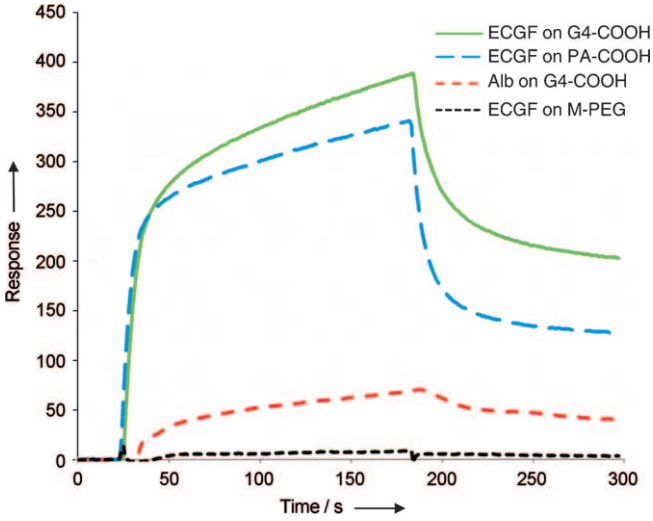

Figure 5. Representative SPR sensorgrams for ECGF binding to NPs modified with the G4-COOH dendrimer (solid green line) and PA-COOH (dashed blue line). Low levels of albumin binding were observed on the G4-COOH-modified NPs (dashed red line). The majority of the ECGF binding is mediated via the NP macromolecular hybrid complex as deduced by the low amounts of ECGF found on the M-PEG control surface (dotted black line).

is also clear that the binding of ECGF to PA-COOH arrays is saturated and dissociates more quickly than the dendrimer-loaded arrays. Repeated injections allowed a higher loading capacity to be reached with dendrimer-coated particles (see the Supporting Information). We expect the high charge density and the branched shape of the dendrimer to be responsible for the differences in the ECGF binding. Albumin only weakly adsorbed when injected onto the dendrimer-coated array in a higher concentration (10 μM/170 $\mu g\,mL^{-1}$).

In conclusion, we have demonstrated a nonlithographic, chemical self-assembly method to form nanopatterns of macromolecules with defined separation versus that on an inert PEG background. The technique can be applied to flat or curved surfaces, and also to sensor surfaces, thereby allowing straightforward quantification of protein binding with a macromolecular array. It was seen by investigating the number and morphology of primary human endothelial cells grown on arrays of dendrimers and linear macromolecules of similar size and charge that the dendrimer potentiated the cell growth to a larger extent than the linear counterpart. We also demonstrated that the macromolecular arrays bind proteins from cell media and that protein binding is dependent on the type of protein and the macromolecular architecture.

Received: October 18, 2010
Revised: January 20, 2011
Published online: March 10, 2011

Keywords: cell adhesion · dendrimers · nanoparticles · self-assembly

[1] a) M. J. Dalby, C. C. Berry, M. O. Riehle, D. S. Sutherland, H. Agheli, A. S. G. Curtis, *Exp. Cell Res.* **2004**, *295*, 387–394; b) H. E. Gaubert, W. Frey, *Nanotechnology* **2007**, *18*, 135101; c) J. Y. Yang, Y. C. Ting, J. Y. Lai, H. L. Liu, H. W. Fang, W. B. Tsai, *J. Biomed. Mater. Res. Part A* **2009**, *90*, 629–640; d) F. Kantawong, K. E. V. Burgess, K. Jayawardena, A. Hart, R. J. Burchmore, N. Gadegaard, R. O. C. Oreffo, M. J. Dalby, *Biomaterials* **2009**, *30*, 4723–4731; e) M. Arnold, E. A. Cavalcanti-Adam, R. Glass, J. Blummel, W. Eck, M. Kantlehner, H. Kessler, J. P. Spatz, *ChemPhysChem* **2004**, *5*, 383–388; f) E. A. Cavalcanti-Adam, A. Micoulet, J. Blummel, J. Auernheimer, H. Kessler, J. P. Spatz, *Eur. J. Cell Biol.* **2006**, *85*, 219–224; g) E. A. Cavalcanti-Adam, T. Volberg, A. Micoulet, H. Kessler, B. Geiger, J. P. Spatz, *Biophys. J.* **2007**, *92*, 2964–2974; h) B. Geiger, J. P. Spatz, A. D. Bershadsky, *Nat. Rev. Mol. Cell Biol.* **2009**, *10*, 21–33.

[2] a) P. Roach, D. Farrar, C. C. Perry, *J. Am. Chem. Soc.* **2005**, *127*, 8168–8173; b) Y. Arima, H. Iwata, *J. Mater. Chem.* **2007**, *17*, 4079–4087; c) K. Rajangam, H. A. Behanna, M. J. Hui, X. Q. Han, J. F. Hulvat, J. W. Lomasney, S. I. Stupp, *Nano Lett.* **2006**, *6*, 2086–2090.

[3] a) D. Page, D. Zanini, R. Roy, *Bioorg. Med. Chem.* **1996**, *4*, 1949–1961; b) S. Hong, P. R. Leroueil, I. J. Majoros, B. G. Orr, J. R. Baker, M. M. B. Holl, *Chem. Biol.* **2007**, *14*, 107–115; c) P. Wu, X. Chen, N. Hu, U. C. Tam, O. Blixt, A. Zettl, C. R. Bertozzi, *Angew. Chem.* **2008**, *120*, 5100–5103; *Angew. Chem. Int. Ed.* **2008**, *47*, 5022–5025.

[4] J. W. Slot, H. J. Geuze, *J. Cell Biol.* **1981**, *90*, 533–536.

[5] A. O. Lundgren, F. Bjorefors, L. G. M. Olofsson, H. Elwing, *Nano Lett.* **2008**, *8*, 3989–3992.

[6] www.polymerfactory.com.

[7] a) M. Malkoch, H. Claesson, P. Lowenhielm, E. Malmstrom, A. Hult, *J. Polym. Sci. Part A* **2004**, *42*, 1758–1767; b) C. C. Lee, J. A. MacKay, J. M. J. Frechet, F. C. Szoka, *Nat. Biotechnol.* **2005**, *23*, 1517–1526; c) C. C. Lee, E. R. Gillies, M. E. Fox, S. J. Guillaudeu, J. M. J. Frechet, E. E. Dy, F. C. Szoka, *Proc. Natl. Acad. Sci. USA* **2006**, *103*, 16649–16654.

[8] R. Vestberg, A. M. Piekarski, E. D. Pressly, K. Y. Van Berkel, M. Malkoch, J. Gerbac, N. Ueno, C. J. Hawker, *J. Polym. Sci. Part A* **2009**, *47*, 1237–1258.

[9] a) H. Ihre, O. L. P. De Jesus, J. M. J. Frechet, *J. Am. Chem. Soc.* **2001**, *123*, 5908–5917; b) M. Malkoch, E. Malmstrom, A. Hult, *Macromolecules* **2002**, *35*, 8307–8314.